Rev.Adv.Mater.Sci. 5 (2003) 348-353

EFFECT OF WORK OF ADHESION ON NANOINDENTATION

Ya-Pu Zhao[1], Xinghua Shi[1] and W. J. Li[2]

[1]LNM, Institute of Mechanics, Chinese Academy of Sciences, Beijing 100080, China
[2]Center for Micro and Nano Systems, The Chinese University of Hong Kong, Shatin, N.T., Hong Kong SAR, China

Received: June 08, 2003

Abstract. Three adhesion contact models, JKR (Johnson-Kendall-Roberts), DMT (Derjaguin-Muller-Toporov) and MD (Maugis-Dugdale) are compared with the Hertz model in dealing with the nano-contact problems. It has been shown that the dimensionless load parameter, $\overline{P}=P/(\pi\Delta\gamma R)$, and the transition parameter, λ, have significant influences on the contact stiffness (contact area) at micro/nano-scale and should not be ignored in shallow nanoindentation.

1. INTRODUCTION

There has been considerable interest in recent years in the mechanical characterization of thin film systems and small volumes of material using depth-sensing indentation tests, which utilize either spherical or pyramidal indenters [1, 2]. Usually, to obtain values for hardness and elastic modulus of the specimen material from experimental values of indenter load and depth of penetration is the principal goal of such testing. The forces involved are usually in the millinewton (10^{-3} N) range and are measured with a resolution of a few nanonewtons (10^{-9} N), and the depths of penetration are in the order of nanometers, hence the term 'nanoindentation (10^{-9} m)'. As the experimental values of indenter load and depth of penetration give an indirect measure of the area of contact, from which the mean contact pressure, and thus hardness, can be estimated, the relationship between the contact area and the load is considerably important. Thus the appropriate use of the corresponding theoretical model will play a key role in the experimental investigation.

Nano-contact mechanics refers to the contact mechanics at nano-scales, which is fundamentally important to understand the force-distance curves of various scanning microscopes (AFM, MMF, etc.) and of nanoindentation, the adhesion (or stiction) of microelectromechanical systems (MEMS) and nanoelectromechanical systems (NEMS), nano-tribology and nano-wear. The emphasis of the present paper is to compare different adhesion contact mechanics models in their dimensionless form, and to discuss the influences of the governing dimensionless parameters.

The influence of the work of adhesion on nano-scale plastic deformation has to be considered for a nanoindentation characterization and modeling. The classical definition of hardness of material is $H=P/A$, and P is the applied load, $A=\pi a^2$ is the contact area, and a is the plastic contact area. Considering the influence of work of adhesion, the relationship between the hardness and the work of adhesion for the contact between a semi-sphere and a semi-infinite plane is [3]

$$P + 2\pi\Delta\gamma R = \pi a^2 H_{ad}, \qquad (1)$$

where R is the radius of the semi-sphere, $\Delta\gamma=\gamma_1+\gamma_2-\gamma_{12}$ is the work of adhesion, γ_1 and γ_2 are the surface energies per unit area of the spherical surface, respectively, and γ_{12} is the interfacial energy. The von Mises yield criterion has been used in the derivation of Eq. (1). Then the nanoindentation hardness con-

Corresponding author: Ya-Pu Zhao, e-mail: yzhao@lnm.imech.ac.cn

© 2003 Advanced Study Center Co. Ltd.

sidering the effect of work of adhesion for fully plastic contact can be expressed as:

$$H_{ad} = H\left(1+\frac{2}{\overline{P}}\right), \tag{2}$$

where $\overline{P}=P/(\pi\Delta\gamma R)$ is the dimensionless load parameter, or the ratio of the applied load and the adhesion force. Eq. (2) shows that the influence of the dimensionless load parameter, $\overline{P}$, on the measured hardness. In other words, the influence of the work of adhesion is strong when the applied load is light.

2. MODELS OF CONTINUUM ADHESION CONTACT MECHANICS

Continuum models that predict the contact area for various geometries have a long history, dating back to the pioneering work of Hertz in 1881 [4]. For simplicity, we consider the contact between a rigid indenter and the elastic semi-infinite plane.

Hertz found that the radius of the circle of contact a_H was related to the indenter load P, the spherical indenter radius R, and the elastic properties of the contacting materials by:

$$a_H^3 = \frac{3PR(1-\nu^2)}{4E}, \tag{3}$$

where E and ν are the Young's modulus and the Poisson's ratio of the test sample. In the absence of adhesion, the Hertz model has been shown to accurately describe the contact area between elastic bodies. However, a great many experimental and theoretical results show that the surface-to-bulk ratio becomes significant at small scales [5]. Therefore, adhesion arising from attractive surface forces is generally not negligible and must be included in any description of contact area (contact stiffness). Actually, with the increasing popularity of nanoscale technology and the increasing sensitivity of nanoindentation instruments, experimental results increasingly show that the contact area of the bodies is much larger than estimated with the Hertz model; especially, when the load diminishes to zero, the contact area reaches a constant value. It proves that the surface forces, especially the adhesion force, do play an important role in the contact of the indenter and the sample at sub-micro/nano scale.

Considering the contact between a rigid sphere with radius, R, and a rigid semi-infinite plane, the adhesion force, P_A, between them is given by the Bradley theory [6] as

$$P_A = 2\pi\Delta\gamma R. \tag{4}$$

Derjaguin, Muller, and Toporov [7] counted for the case of deformable bodies by adding the force given by Eq.(4) to the Hertz contact equations and the resulting contact theory is referred to as the 'DMT' theory. The DMT model gives the contact radius a_{DTM} related to the work of adhesion, $\Delta\gamma$, by:

$$a_{DMT}^3 = \frac{3R(1-\nu^2)}{4E}(P+2\pi\Delta\gamma R). \tag{5}$$

It is obvious that upon a negative load, $P_{c(DMT)}$ is given by:

$$P_{c(DMT)}=-2\pi\Delta\gamma R. \tag{6}$$

the contact radius is zero which means two surfaces separate on that point. Therefore, $P_{c(DMT)}$ is the critical force required to separate the two spheres, i.e., the pull-off force.

The adhesion contact between a solid rigid sphere and an elastic half space has been treated by Johnson, Kendall and Roberts (JKR), which leads to the famous JKR theory [8]. They found that the contact radius, a_{JKR}, for a rigid sphere in contact with a compliant elastic half space, was related to the work of adhesion, $\Delta\gamma$, as:

$$a_{JKR}^3 = \frac{3R(1-\nu^2)}{4E}\times \left\{P+3\pi\Delta\gamma R+\left[6\pi\Delta\gamma RP+(3\pi\Delta\gamma R)^2\right]^{1/2}\right\}. \tag{7}$$

According to the JKR theory, upon application of a negative load, separation of the surfaces would occur when the external force, $P_{c(JKR)}$, was applied such that

$$P_{c(JKR)} = -\frac{3}{2}\pi\Delta\gamma R. \tag{8}$$

It should be noted that the pull-off force $P_{c(JKR)}$ is independent of the elastic modulus and depends only on the radius of sphere and work of adhesion. So Eq.(8) should apply equally well to a rigid sphere, but this would be contradictory to Eq.(4). The apparent discrepancy led to a heated debate and later, following the analysis of Tabor [9], Muller *et al*. [10] pointed out that the two theories represented the opposite extremes of a dimensionless parameter μ given by

$$\mu = \left(\frac{R\Delta\gamma^2(1-\nu^2)}{E^2\varepsilon^3}\right)^{1/3}, \tag{9}$$

Table 1. Comparison of the various contact theories .

Theory	*Assumptions*	*Limitations*
Hertz	No surface forces.	Not appropriate for low loads if surface forces presents.
JKR	Short-ranged surface forces act only inside contact area. Contact geometry allowed to deform.	May underestimate loading due to surface forces. Applies to high λ systems only.
DMT	Long-ranged surface forces act only outside contact area. Geometry constrained to be Hertz.	May underestimate contact area due to restricted geometry. Applies to low λ systems only.
Maugis-Dugdale	Periphery of tip-sample interface modeled as a crack that failed at its theoretical strength.	Solution analytical, but parametric equations. Applies to all values of λ.

where ε is the equilibrium spacing in the Lennard-Jones potential. The significance of the Tabor number μ in the contact theory, especially at the nanoscale, has attracted attention by many researchers (e.g. [5]). ε can be interpreted as the ratio of elastic deformation resulting from adhesion to the effective range of surface forces. Another dimensionless number, called transition parameter λ, was introduced by Maugis [11], and the transition parameter is related to μ by λ=157μ. For an appropriate use of the adhesion models, an adhesion map has been constructed by Johnson and Greenwood [12] using the Dugdale force-separation law with two parameters: μ (or λ) and $\overline{P}$, where the dimensionless load parameter $\overline{P}$ is the ratio of the applied load to the adhesion force. The JKR theory is applicable to large radius compliant solids (μ > 5) and the DMT theory applies to small radius rigid solids (μ <0.1). Physically, the JKR theory accounts for adhesion forces only within the expanded area of contact, whereas the DMT theory accounts for adhesion forces only just outside the contact circle. Table 1 represents the major assumptions and limitations inherent to each theory.

3. COMPRAISON OF THE CONTACT STIFFNESS OF VARIOUS MODELS

To compare the JKR model with the Hertz model, especially the influence of the adhesion force on the contact stiffness, *S*, it is convenient to make Eq. (7) dimensionless as

$$\frac{S_{JKR}}{S_H}=\frac{a_{JKR}}{a_H}=\left\{1+\frac{3}{\overline{P}}+\left[\frac{6}{\overline{P}}+\left(\frac{3}{\overline{P}}\right)^2\right]^{1/2}\right\}^{1/3}, \quad (10)$$

which is always larger than (or equal to) unity as expected. The dimensionless load parameter $\overline{P}$ dominates the change in the contact radius (contact stiffness) in the JKR model. The radius a_{JKR} increases with the work of adhesion $\Delta\gamma$ and with decreasing applied load. This has been discussed in Yang's work [13]. However, there is no such analysis about the DMT model. Division of Eq. (5) by Eq. (3) yields

$$\frac{S_{DMT}}{S_H}=\frac{a_{DMT}}{a_H}=\left(1+\frac{2}{\overline{P}}\right)^{1/3}. \quad (11)$$

From Eq. (11), we know that the contact stiffness (contact radius) also increases with the work of adhesion and with decreasing applied load, as in the JKR model.

Fig. 1a shows that the indentation radius is controlled by the work of adhesion when the load is less than 10^{-3} mN. For a nanoindentation tip radius 1 μm, and the work of adhesion between the tip and film, 100 mJ/m^2, the ratio a_{JKR}/a_H in the JKR model decreases from 12.4 at the applied load 1 nN to 1.5 at load of 1 μN, and in the DMT model, the ratio a_{JKR}/a_H decreases too from 8.6 at the load of 1 nN to 1.2 at the load of 1 μN. Gradually, the ratios for both models reach the value of 1 as the load approaches 1 mN. At small loads, the radius increases sharply with the work of adhesion. It proves that under small loads, the contact radius is dominated by the work of adhesion and the tip radius *R*. Under large loads, the work of adhesion is negligible compared to the strain energy, which controls the deformation of the specimen surface. In conclusion, both in JKR and DMT models, for a small load and a

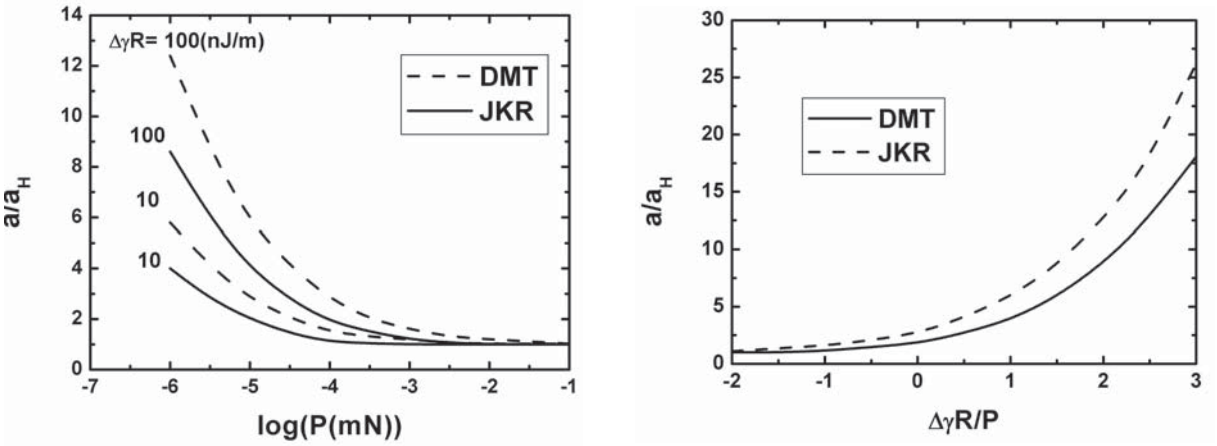

Fig. 1. (a). Influence of work of adhesion $\Delta\gamma$, and applied load P on nanoindentation tip radius ratio in both JKR and DMT models; (b) Influence of dimensionless number $\Delta\gamma R/P$ on nanoindentation tip radius ratio in both JKR and DMT models.

large indenter size, the change in work of adhesion controls the contact radius between the indenter and the substrate. On the contrary, for a large load and small size of the indenter, the elastic deformation dominates.

Also, from Eqs. (10) and (11), it can be seen that the dimensionless load parameter, $\overline{P}=P/(\pi\Delta\gamma R)$, independently controls the influence of the work of adhesion. In Fig. 1b, when the value of $\Delta\gamma R/P$ is less than 0.1, the influence of the work of adhesion is still insignificant. With the value increasing to 10^2, the corresponding value is so large that the work of adhesion must not be ignored and would play the main role in the process of contact.

It should be noted that, in Figs. 1a and 1b, with the same parameter $\Delta\gamma$R, the values denoted by the dashed curve is always larger than that of the solid curve at most sites, which means that the influence of work of adhesion in JKR model is more prominent than the DMT model. Actually, dividing Eq.(7) by Eq.(5), the ratio between a_{JKR} and a_{DMT} is given as:

$$\frac{S_{JKR}}{S_{DMT}}=\frac{a_{JKR}}{a_{DMT}}= \left\{\frac{1+3/\overline{P}+\left[6/\overline{P}+(3/\overline{P})^2\right]^{1/2}}{1+2/\overline{P}}\right\}^{1/3}. \quad (12)$$

From Eq. (12) and Fig. 2, we know that with increasing work of adhesion, the JKR model has more influence on the contact stiffness (contact radius). Also, an ultimate value, $\sqrt[3]{3}$, can be deduced with the decrease of applied load.

4. COMPRAISON OF THE MD MODEL WITH THE HERTZ MODEL

By using the Dugdale model, Maugis proposed the MD model [11] and described the adhesion force between the tip and the sample by a pair-wise summation of the molecules *via* a Lennard-Jones potential. In the MD model, it is found that such model is the general case in describing the contact and both the JKR and DMT models were special cases. The transition between the JKR and DMT models was investigated by Maugis and Gauthier-Manuel [14], who used the 'Dugdale' (square well) potential to describe attractive forces between contacting spheres and obtained the following equations:

$$\frac{1}{2}\lambda\bar{a}\left[\sqrt{m^2-1}+(m^2-2)\arccos(1/m)\right]+ \frac{4}{3}\lambda^2\bar{a}^2\left[\sqrt{m^2-1}\arccos(1/m)-m+1\right]=1, \quad (13)$$

$$\overline{P}=\bar{a}^3-\lambda\bar{a}^2\left[\sqrt{m^2-1}+m^2\arccos(1/m)\right], \quad (14)$$

where $\bar{a}/a=\left(K/\pi\Delta\gamma R^2\right)^{1/3}$, $\bar{c}/c=\left(K/\pi\Delta\gamma R^2\right)^{1/3}$, $m=c/a$, $\overline{P}=P/\left(\pi\Delta\gamma R^2\right)^{1/3}$, and c is the outer radius given as $c=a+0.97\varepsilon$.

It is difficult in the MD model to obtain the explicit expression relating a and P as was the case in JKR and DMT models, because there is another parameter that varies with λ. It is necessary to use numerical calculations to obtain the solution. From

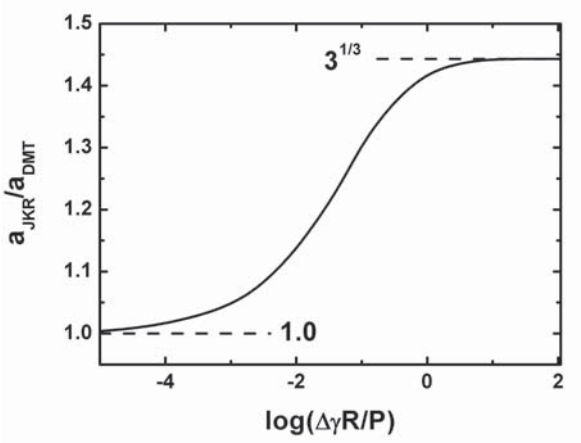

Fig. 2. The ratio of a_{JKR} to a_{DMT} *vs* the dimensionless number $\Delta\gamma R/P$. When the value of increases, the ratio would increases from the lower critical value to the upper one. The lower critical value, 1.0, shows that when surface energy can be ignored, the contact radii in both JKR and DMT models are similar. Actually they are similar to what the Hertz model predicted. The upper critical value, $3^{1/3}$, however, shows the difference of contact radius between the JKR and the DMT models.

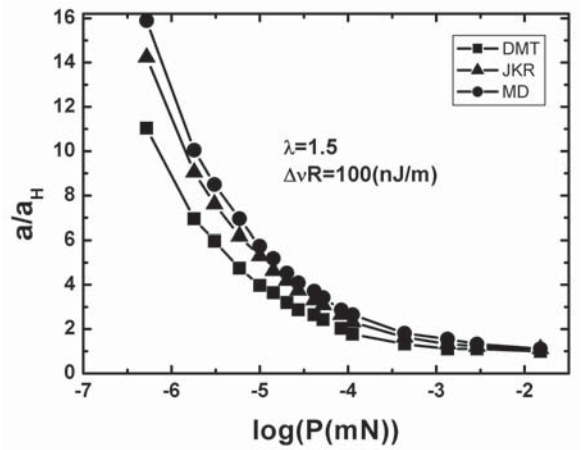

Fig. 3. Effect of applied load *P* on nanoindentation tip radius ratio in JKR, DMT and MD models when λ=1.5 and $\Delta\gamma R$=100 nJ/m.

Fig. 3 for λ = 1.5, the MD curve is in between the JKR and DMT curves. The conclusion about the transition between the JKR model and the DMT model can be verified numerically. When λ = 0.1, the curve for the MD model approaches the curve due to the DMT model and in the case λ = 5, the curve for the MD model approximately coincides with that for the JKR model. So, the JKR and the DMT models are two special cases of the MD model.

5. CONCLUSION

The influences of the dimensionless load parameter, $\overline{P}=P/(\pi\Delta\gamma R)$, and the transition parameter, λ, on the nanoscale contact area (contact stiffness) have been analyzed and the importance of the work of adhesion for shallow nanoindentation has been validated through comparison of the JKR, DMT and MD models with the Hertz model. With a small applied load, the work of adhesion does play a key role in the contacting and is sure indispensable. The difference between the JKR and DMT models is also discussed and the essence of the difference is brought forward. The numerical examples show that both the JKR and DMT models are, respectively, the upper and lower limits of the MD model. So the MD model is the general case and can deal with most materials in contact. A large body of experiment results [15] showed that, in general, the atomic force microscopy (AFM) measurements were mostly located in the regime of the MD model. So considering the accuracy of the experiments, it is more suitable to use the MD model to deal with the problem.

There is no doubt that as the scale of mechanisms becomes smaller, interest in mechanical properties on a nanometer scale and smaller, and the effect of surface forces and adhesion, will continue to increase [1]. The so-called 'pico-indenter' with combination of the nanoindenter and the AFM would be the case that adhesion and surface forces play more important role.

ACKNOWLDGEMENTS

This research was sponsored by the Distinguished Young Scholar Fund of NSFC (Grant No. 10225209), key project from the Chinese Academy of Sciences (Grant No. KJCX2-SW-L2) and National "973" Project (No. G1999033103).

REFERENCES

[1] A.C. Fischer-Cripps, *Nanoindentation* (Springer-Verlag, New York, 2002).
[2] V. Domnich and Y. Gogotsi // *Rev. Adv. Mater. Sci.* **3** (2002) 1.
[3] S.K.R. Chowdhury and H. M. Pollock // *Wear* **66** (1981) 307.
[4] H. Hertz //*J. Reine Angew. Math.* **92** (1881) 156.
[5] Y.P. Zhao, L. S. Wang and T. X. Yu // *J. Adhesion Sci. Technol.* **17** (2003) 519.

[6] R.S. Bradley // *Phil. Mag.* **13** (1932) 853.
[7] B.V. Derjaguin, V.M. Muller and Y.P. Toporov // *J. Colloid Interface Sci*. **53** (1975) 314.
[8] K.L. Johnson, K. Kendall and A.D. Roberts // *Proc. R. Soc. London* **A324** (1971) 301.
[9] D. Tabor // *J. Colloid Interface Sci.* **58** (1977) 2.
[10] V.M. Muller, V.S. Yushchenko and B.V. Derjaguin // *J. Colloid Interface Sci*. **77** (1980) 91.
[11] D. Maugis // *J. Colloid Interface Sci.* **150** (1992) 243.
[12] K.L. Johnson and J.A. Greenwood // *J. Colloid Interface Sc*i. **192** (1997) 326.
[13] F.Q. Yang // *Appl. Phys. Lett.* **80** (2002) 959.
[14] D. Maugis and B. Gauthier-Manuel // *J. Adhesion Sci. Technol*. **8** (1994) 1311.
[15] B. Cappella and G. Dietler // *Surface Sci. Reports* **34** (1999) 1.